ASEAN Engineering Journal

Full Paper

CATHODIC AND ANODIC PLASMA ELECTROLYSIS ON NITRATE SYNTHESIS

Harianingsih[a*], Arief Arfriandi[b], Sri Handayani[c], Maharani Kusumaningrum[a], Amadea Vaskallya Pramesti[a], Faizya Pinka Maharani[a], Nelson Saksono[d]

[a]Department of Chemical Engineering, Faculty of Engineering, Universitas Negeri Semarang, Kampus Sekaran, Gunungpati, Semarang 50229, Indonesia
[b]Department of Electrical Engineering, Faculty of Engineering, Universitas Negeri Semarang, Kampus Sekaran, Gunungpati, Semarang 50229, Indonesia
[c]Department of Civil Engineering, Faculty of Engineering, Universitas Negeri Semarang, Kampus Sekaran, Gunungpati, Semarang 50229, Indonesia
[d]Department of Chemical Engineering, Faculty of Engineering, Universitas Indonesia, Kampus Baru UI, Depok 16242, Indonesia

Article history
Received
02 November 2023
Received in revised form
29 February 2024
Accepted
07 March 2024
Published online
31 August 2024

*Corresponding author
harianingsih@mail.unnes.ac.id

Graphical abstract

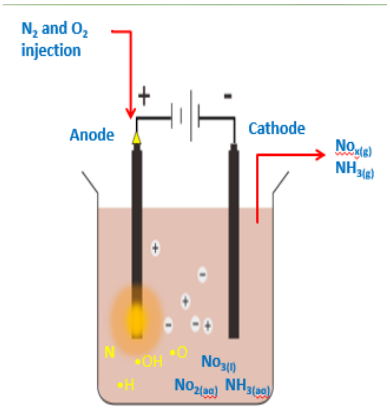

a. Plasma electrolysis reactor

Abstract

Nitrogen fixation using plasma electrolysis is an alternative in the production of liquid nitrate fertilizer which is safe for the environment because it does not produce emissions that pollute the environment. The effectiveness of nitrate production is shown from the position of plasma formation at cathodic and anodic levels. This study aims to analyze the comparison of cathodic and anodic plasma electrolysis levels in producing nitrate. Current-voltage characterization is carried out to determine the position of plasma formation. The glow discharge of the cathodic plasma is achieved after the critical voltage (280 V) is lower than that of the anodic plasma (650 V). Measurement of emission intensity using electron spin resonance to determine reactive species that play a role in the formation of nitrate in cathodic and anodic plasma. Nitrate formation is influenced by reactive species in the form of N, N_2*, N_2^+, •OH, •H and •O, especially reactive species of nitrogen and •OH are needed to form nitrate both from the NO pathway (anodic plasma) and from the ammonia pathway (cathodic plasma). The results of this study showed that anodic plasma electrolysis was more effective for nitrate synthesis. Nitrate produced from anodic plasma is 1889 mg L^{-1}, greater than cathodic plasma as much as 213 mg L^{-1}.

Keywords: critical voltage, emission intensity, glow discharge, nitrate fertilizer, reactive species

1.0 INTRODUCTION

Nitrate synthesis has been carried out using various nitrogen fixation methods, both natural and industrial. In natural nitrogen fixation, nitrate synthesis occurs through a nitrification process, in which nitrifying bacteria convert ammonia into nitrate, which is then absorbed by plants [1]. Although plants absorb nitrate from the nitrification process, the amount is not sufficient for plant nitrogen needs, ranging from 100-250 mg L^{-1} [2]. On the other hand, nitrogen fixation on an industrial scale involves the conventional Haber-Bosch method. This process produces ammonia through the fixation of nitrogen and hydrogen at high temperatures and pressures. However, the Haber-Bosch process requires energy in the steam reforming process to produce hydrogen gas from CH_4 natural gas, causing large CO_2 emissions [3]. This process also causes significant energy consumption and use of natural gas, and produces about 300 million tonnes/year of carbon dioxide. In addition, ammonia itself contributes to 75 % of greenhouse gas emissions [4]. On the other hand, nitrogen fixation on an industrial scale involves the conventional Haber-Bosch method. This process produces ammonia through the fixation of nitrogen and hydrogen at high temperatures and pressures. Air plasma technology is emerging as an environmentally friendly alternative in nitrate production [5]. This process has a much lower energy consumption than the Haber-Bosch method, about 2.5 times lower [6]. However, air plasma technology has problems in producing sufficient nitrate yield in liquid form. Nitrate is needed by plants in liquid form, but the diffusion of NO and NO_2 gases produced from air plasma into the liquid phase is still limited, inhibiting the formation of NO_3^-. In addition, the amount of •OH and •H

required for the formation of nitrate is still limited [7]. NO_2 which is in the soluble gas phase reacts with NO and •O species reactives, causing a shift in the equilibrium in solution towards NO_2, so that the NO_3^- formed may change to NO_2 to reach equilibrium [8].

One approach to overcome the problem of low nitrate production from air plasma technology is to use the plasma electrolysis method. This method involves plasma formed in solution with reactive species capable of converting N_2 and O_2 from air into NO_x and nitrate compounds [9]. Synthesis of liquid nitrate by plasma electrolysis using air as the main source of nitrogen is promising, although it requires a deeper understanding so the purpose of this study is to analyze the effect of plasma formation at the cathode and anode on nitrate production. In addition, this study also aims to determine the emission intensity of the formation of reactive species which is dominated by the role of •OH which oxidizes and then forms NO_3^- quickly [10].

2.0 METHODOLOGY

2.1. Materials

The materials used in this study included air injection with flowrate 0.8 $Lmin^{-1}$, Potassium sulfate MERCK 1.05153.0500 dissolved in distilled water as an electrolyte, and nitrate test reagent HACH 2106169. In addition, materials such as cadmium sulfate hydrate MERCK 1.02027 were used in the analysis of nitrite. Copper (II) sulfate pentahydrate MERCK 1.02790.1000, and N-(1-naphythyl)-ethylenediamine dihydrochloride (NED) MERCK 106237. The reactor used has a cylindrical shape and is made of glass, with a volume capacity of 1.2 L.

2.2. Experimental

This reactor is equipped with various devices such as temperature sensors, condensers, power analyzers, AS SUS 316 type stainless steel electrodes with a diameter of 5 mm, and tungsten type EWTH-2 RHINO GROUND measuring 1.6 mm x 175 mm. Energy is provided by a voltage power supply, which can adjust the voltage from 0 to 1000 V and the current strength in the range of 0 to 5 A. Several other instruments used in this study include a UV-VIS spectrophotometer (BEL Engineering UV-M51 Single Beam Spectrophotometer) to analysis of nitrate. Measurement of the intensity of the emission spectrum was carried out using an ESR (Electron Spin Resonance) connected to an optical probe. This process was carried out in a dark room to identify gas formed in the reactor, especially due to plasma discharge at the electrodes. This aims to eliminate interference from other light waves that can be received by the camera, considering that this device is set in the wavelength range of 200 to 1100 nm with a very high UV-NIR sensitivity response. Furthermore, within the framework of this research, an Intensified CCD (Intensified Charge Coupled Divice) camera is used vertically against the plasma splash. Fixed signal pickup at 1 ms time interval.

2.3. Procedure

The procedure from the research shown in Figure 1.

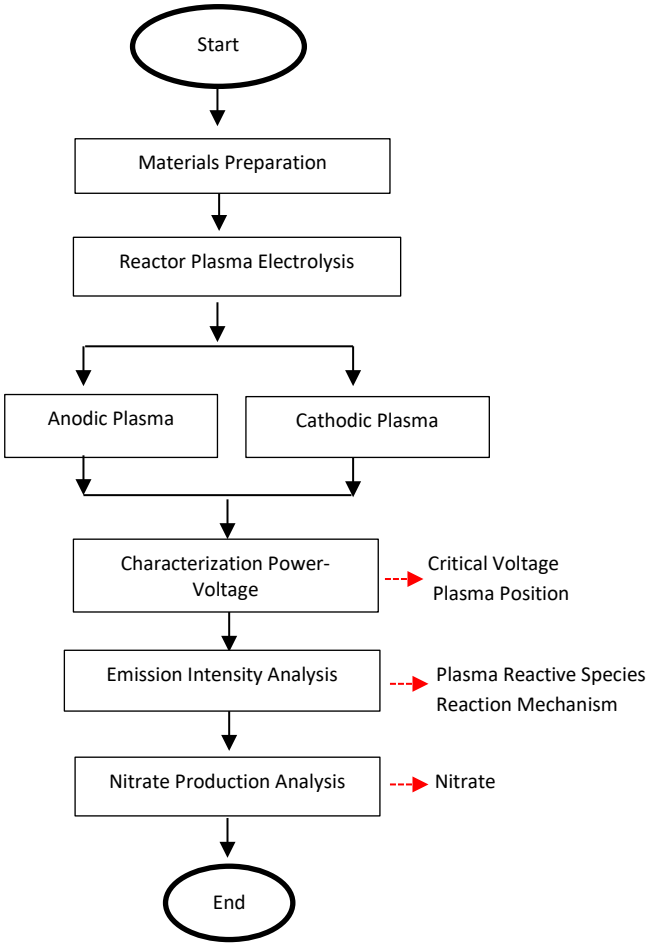

Figure 1 Research Workflow

2.3.1.Plasma Electrolysis Reactor Performance Test

Before synthesizing liquid nitrate fertilizer using a plasma electrolysis reactor, it is necessary to first test the reactor performance. The test was carried out to obtain the characteristics of the plasma formed in the glow discharge zone with a certain voltage range. For every 20 volt increase in voltage, the current value is measured and the data is taken. If the current value obtained fluctuates. then the current value is recorded for 1 minute and then the average value is taken. Even more so. current measurement data can be used to create a curve of the voltage range used in increments of 20 V to the current. Plasma characterization tests were carried out at electrolyte concentrations using 0.02 M of K_2SO_4. The voltage and current range values in the glow discharge zone can be seen by the larger and more stable plasma that is formed when the current and voltage are directly proportional again.

2.3.2.Reactive Species Emission Intensity Analysis

For reactive species tests. Electron Spin Resonance (ESR) can be used. The reactor containing the nitrate sample was inserted into a main unit that connected a wavelength-matched optical phrobe to a personal laptop with radical species analysis software installed. The emission spectrum graphic display can be seen on the personal computer screen.

2.3.3. Nitrate Analysis

Prepare 25 mL of test sample into a 100 mL volumetric flask. Add 5 g of Nitraver 5 Nitrate Reagent Powder Pillow HACH 2106169 then shake. Pass the solution through the reduction column with a flow rate of 7 - 10 mL min^{-1}. Measure the absorption between 10 minutes and 2 hours after adding the dye solution at a wavelength of 543 nm to the spectrophotometer. Determine the total nitrite content from the calibration curve. The measured level is the total nitrite level which comes from nitrite and nitrate which have been reduced to nitrite. Testing nitrite separately was carried out on 50 mL of the same test sample (without going through the reduction column).

3.0 RESULTS AND DISCUSSION

In this study, the electrolyte solution was prepared using K_2SO_4. The cathode was constructed from stainless steel, while the anode was made from tungsten. Both of these electrode materials are inert, meaning they do not undergo significant chemical reactions during the electrolysis process. This selection of materials ensures that the reactions occurring are primarily driven by the electrolysis of the K_2SO_4 solution and the subsequent formation of reactive species. The introduction of gas through air injection, at a rate of 0.8 L min^{-1}, directly into the electrode area plays a significant role in facilitating the ionization process during plasma formation. This action has the effect of decreasing the energy consumption necessary for the evaporation process, typically achieved through Joule heating. By enhancing the ionization process, the plasma formation becomes more efficient, leading to reduced energy requirements for vaporization. Furthermore, the mechanics of gas injection and the specific rate of gas flow have a direct impact on the physical and chemical characteristics of the resulting plasma. The manner in which gas is injected and the rate at which it flows contribute to shaping the properties of the plasma formed. These factors influence the plasma's temperature, composition, reactivity, and overall behavior. In essence, the controlled addition of gas, such as air injection, provides a strategic means to optimize the plasma formation process, enhancing its efficiency and characteristics while simultaneously mitigating energy consumption associated with Joule heating and evaporation [11].

3.1. Plasma Formation Position

Plasma electrolysis can form on both the anode and cathode sides, with smaller surface areas tending to form plasma. The production of reactive hydroxyl species is more dominant in anodic plasma electrolysis, while more reactive hydrogen species are produced in cathodic plasma electrolysis [12] . The location of plasma formation also affects the types of compounds formed as a result of electrochemical reactions. Visually, the difference in the color of the solution can be observed, where the color of the anodic plasma solution tends to be clearer than the color of the solution in the cathodic plasma which is more turbid (Figure 2 (a) and (b). In plasma electrolysis, a direct current is produced between the electrode and the surface of the surrounding K_2SO_4 electrolyte solution [13]. Bubbles form around the electrode cell and the increased heat causes evaporation of the electrolyte solution so that a sheath forms around the electrode. In addition to the visual differences in electrolyte solutions, anodic and cathodic plasmas also differ in current-voltage characteristics [14].

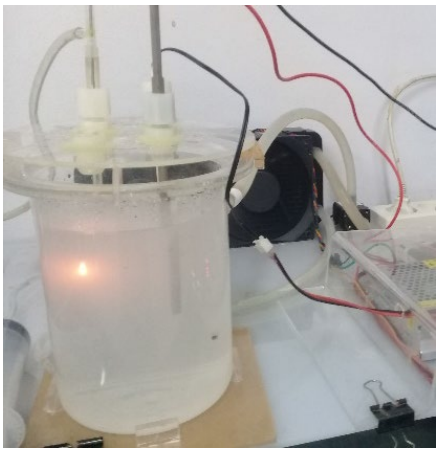

(a)

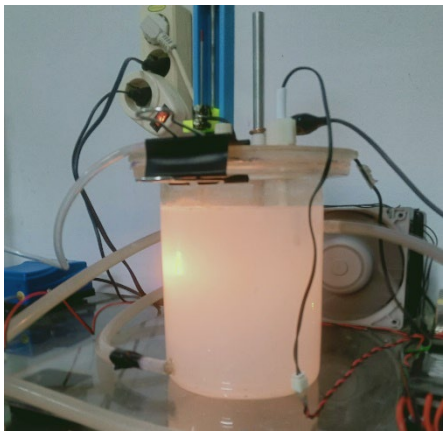

(b)

Figure 2 Visualization of Anodic Plasma (a) and Cathodic Plasma (b)

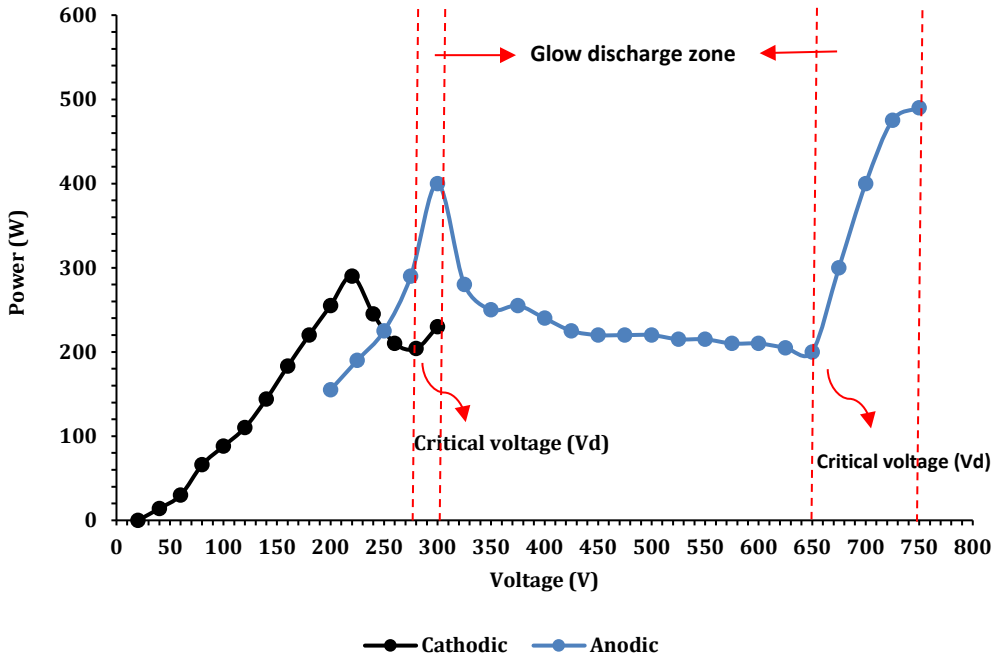

Figure 3 The cathodic and anodic plasma critical voltage

In nitrate fixation using plasma electrolysis, many reactive species are formed in the glow discharge zone. The plasma glow discharge zone in this study begins after reaching a critical voltage (Vd). The critical voltage is the minimum voltage required to form a stable plasma, so that plasma is more easily formed in cathodic plasma. In this zone there are many reactive species that are produced so that they can produce nitrate. The critical voltage which continues to increase causes the electric current to increase so that the power also increases, the plasma light gets brighter [15]. Based on Figure 3, the current-voltage curve in cathodic plasma explains that the formation of a critical voltage is relatively lower than in anodic plasma. The cathodic plasma has the limitation that after a critical voltage, the stable plasma zone cannot be reached for a longer time and at a higher voltage [16]. The critical voltage of the cathodic plasma (280 V) is lower than that of the anodic plasma (650 V). This is due to the ease of formation of the gas sheath at the anode, which is more volatile than at the cathode. The end layer of the electrode is also eroded more quickly. This condition occurs because the reaction zone that occurs in the cathodic plasma is dominated by the plasma phase, very little occurs on the surface between the plasma and the electrolyte [17]. The large electron emission coefficient causes relatively more excited electrons on the cathode surface which has an impact on reducing the number of energy electrons entering the reaction zone of the plasma-electrolyte interface layer, resulting in a significant reduction in energy around the cathode surface. In contrast to anodic plasma where the reaction zone is dominated at the plasma-electrolyte interface area so that the critical voltage is larger [18].

3.2. Cathodic and Anodic Plasma Reactive Species

The reactive species are the main oxidizing and reducing agents used in the synthesis of nitrates [19]. Uncharged reactive species are formed due to the breaking of paired electron bonds in a molecule. The type and amount of reactive species generated in the plasma electrode will affect the speed of achieving plasma stability [2]. The findings of this study highlight that the creation of nitrate is impacted by various reactive species, encompassing N, N_2*, N_2^+, •OH, •H, and •O. Nitrogen and hydroxyl (•OH) reactive species play roles in the nitrate formation process, contributing to both the NO pathway (associated with anodic plasma) and the Ammonia pathway (associated with cathodic plasma). The generation of these reactive species is subject to the quantity of nitrogen and oxygen introduced into the plasma electrolysis reactor. Notably, the emission of N_2*, •O, •H, and •OH reactive species stands out as the predominant chemical entities within plasmas produced in atmospheric pressure electrolyte solution [13].

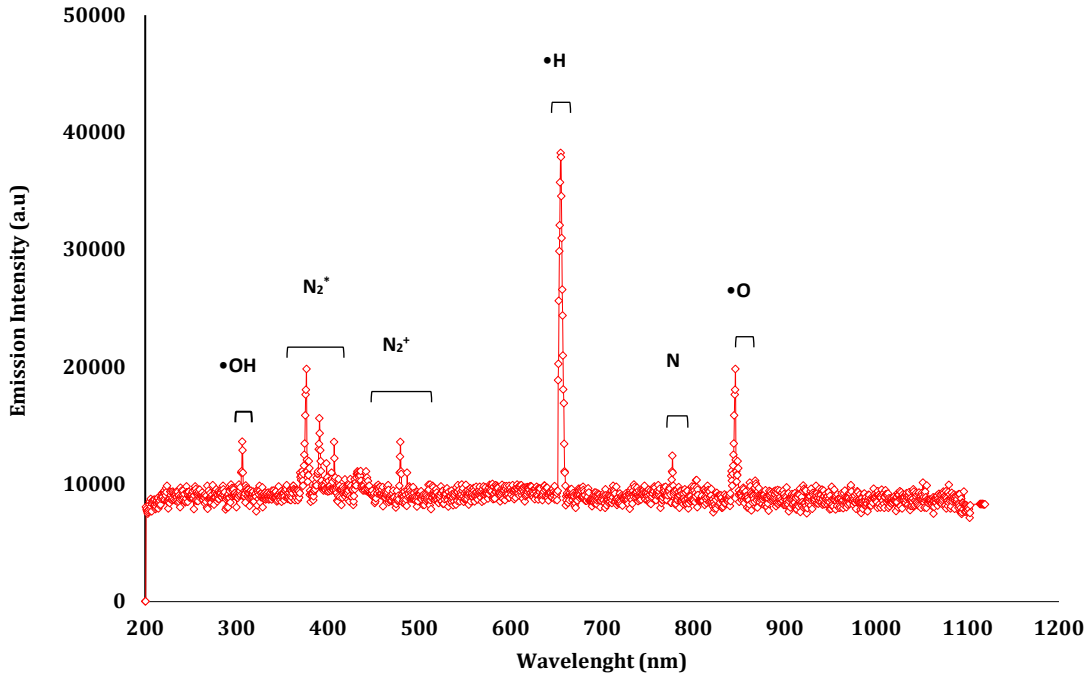

Figure 4 Emission intensity of cathodic plasma

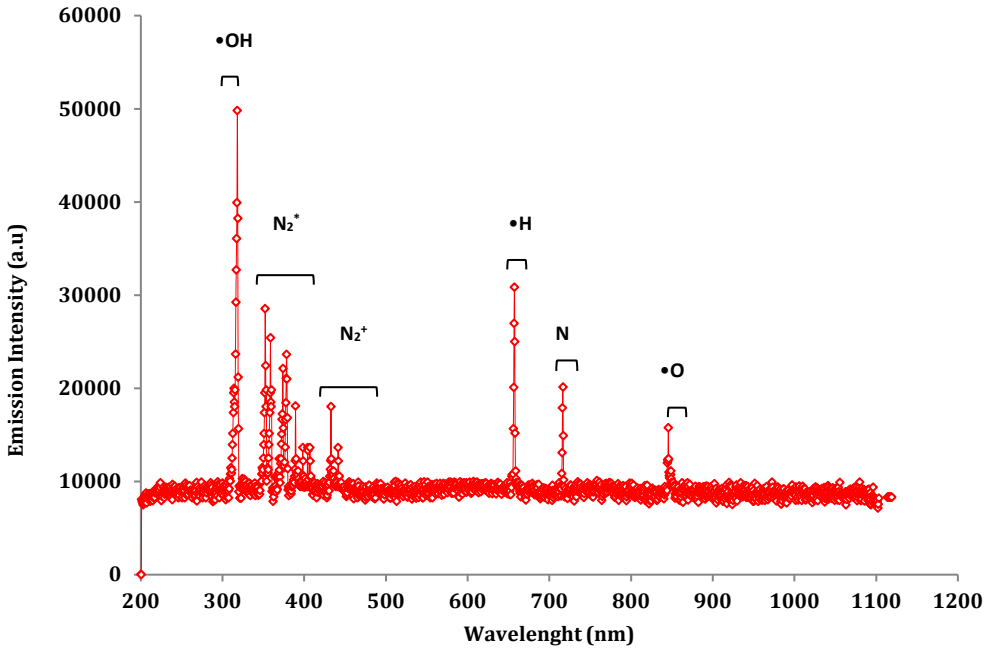

Figure 5 Emission intensity of anodic plasma

In Figures 4 and 5, reactive species in the form of •N, •N_2*, •N_2^+, •OH, •H and •O that the absorbance of unit shown in table 1, especially reactive •species H and •OH are required to form nitrate either from the NO pathway or from the ammonia pathway in cathodic and anodic plasma. When plasma is generated in an electrolyte solution at atmospheric pressure it generates high energy electrons which can effectively ionize air molecules. •N_2*, •H and •OH emissions were identified as the predominant species in plasma generated in atmospheric pressure electrolyte solutions [20]. The formation of •OH and •H apart from injection is also produced by the dissociation of H_2O. Cathodic plasma reduction leads to the conversion of H_2O into hydrogen gas (H_2), subsequently decomposed into •H radicals. Conversely, during anodic plasma, the primary reaction involves ionizing H_2O to generate hydroxyl radicals •OH. Plasma tends to be more readily generated and stable within the gas phase, and the presence of H_2 gas aids in stabilizing the cathodic plasma. In contrast, in anodic plasma, the hydroxyl radical •OH recombines, yielding H_2O_2 which exhibits high solubility in water. Anodic plasma refers to the plasma generated at the anode, achieved by minimizing the anode's contact area within the solution relative to the cathode [21]. This segment will elaborate on the impact of various process variables on the concentration of the K_2SO_4 electrolyte solution, the rate of air injection, and shifts in operational temperature. The

introduction of solute results in an increased evaporation load on the anode, demanding a higher voltage for maintaining plasma stability in the anodic plasma. The reactive species •OH promptly recombine to form uncharged hydrogen peroxide. Plasma electrolysis produces two distinct reaction zones: 20% of •OH formation takes place within the plasma phase zone, while the remaining 80% occurs in the liquid phase reaction zone at the plasma-electrolyte interface [22]. Within the plasma phase reaction zone, H_2O vapor molecules dissociate into H_2 and O_2 following equations (1)-(7) [23].

$$H_2O_{(l)} + e^- \rightarrow \bullet OH + \bullet H + e^- \quad (1)$$

$$H_2O + e^- \rightarrow 2e^- + H_2O^+ \quad (2)$$

$$H_2O^+ + H_2O \rightarrow \bullet OH + H_3O^+ \quad (3)$$

$$H_2O + e^- \rightarrow H_2O^* + e^- \quad (4)$$

$$H_2O^* + H_2O \rightarrow H_2O + \bullet OH + \bullet H \quad (5)$$

$$H_2O^* + H_2O \rightarrow H_2 + \bullet O + H_2O \quad (6)$$

$$H_2O^* + H_2O \rightarrow 2\bullet H + \bullet O + H_2O \quad (7)$$

Within the liquid phase reaction zone adjacent to the plasma-electrolyte interface, certain liquid H_2O molecules engage in reactions with H_2O^+ ions emanating from the plasma zone in close proximity to the electrodes. This interaction results in the creation of H_2, along with the generation of H_2O_2 and O_2 [24].

$$\bullet N + \bullet H \rightarrow \bullet NH \quad (8)$$

$$\bullet NH + \bullet H \rightarrow \bullet NH_2 \quad (9)$$

$$\bullet NH_2 + \bullet H \rightarrow NH_3 \quad (10)$$

Equation (8)-(9) shown that the potential mechanism for the formation of •N and •H reactive species, leading to nitrate production via the ammonia pathway, involves the active participation of reactive species •OH. Among these, •OH facilitates the oxidation process of NH_4^+ into NH_3, reducing the ammonium content and enabling the rapid formation of NO_3^- [25]. In Figure 5, when an air injection flowrate of 0.8 $Lmin^{-1}$ is combined with an electrolyte concentration of 0.02 M of K_2SO_4, an optimal equilibrium is achieved between electric power and air injection. This balance results in the generation of various reactive species, including •OH, •N, •N_2*, •N_2^+, •H, and •O. Emission spectrum analysis is performed within a dark environment to identify the gases produced within the reactor as a result of plasma discharge at the electrodes. This approach eliminates interference from other light sources, as the equipment is finely tuned to a wavelength range of 200–1100 nm with heightened UV-NIR sensitivity [26]. In this study, an Intensified Charge Coupled Divide (ICCD) camera is positioned perpendicular to the plasma splashes, with a fixed signal time of 1 millisecond. The resulting light spectrum from the plasma discharge is translated into a graph spanning 300–850 nm. Notable spectral lines include •OH (308 nm), •N_2* (317, 337, 380, 399 nm), •N_2^+ (427, 479 nm), •H (654 nm), •N (777 nm), and •O (844 nm). Across diverse camera positions, the emission spectrum primarily showcases excited nitrogen molecules (•N_2*), a consequence of high-energy electron collisions with N_2 and O_2 molecules.

Table 1 Emission Intensity (absorbance of unit reactive species) and nitrate production

Plasma Position	Emission Intensity of Reactive Species (a.u)						Nitrate (mg L^{-1})
	•N	•N_2*	•N_2^+	•OH	•H	•O	
Cathodic	11098	18450	14300	12600	38200	18405	213
Anodic	20139	28540	18023	49800	12547	17890	1889

Table 1 presents a comparison of nitrate production levels between anodic plasma (1889 mg L^{-1}) and cathodic plasma (213 mg L^{-1}). The roles of reactive species, including •OH, •N, •N_2*, •N_2^+, •H, and •O, align with the equations described in the literature, specifically equation 16-18 [27], 19-21[8], 22-27 [17]. These equations provide theoretical frameworks that explain the involvement of these reactive species in the observed nitrate production processes within the plasma electrolysis setup. The differences in nitrate production between anodic and cathodic plasma align with the expected roles of these reactive species as outlined in the referenced literature.

$$N_2 + e^- \rightarrow \bullet N + \bullet N + e^- \quad (11)$$

$$O_2 + e^- \rightarrow \bullet O + \bullet O + e^- \quad (12)$$

$$\bullet O + H_2O_{(l)} \rightarrow \bullet OH + \bullet OH \quad (13)$$

$$H_2O_{(l)} + e^- \rightarrow \bullet H + \bullet OH + e^- \quad (14)$$

$$N_{2(g)} + H_2O_{(l)} \rightarrow \bullet N_2^+ + \bullet OH + \bullet H \quad (15)$$

$$N_{2(g)} + \bullet O \rightarrow NO + \bullet N_2^* \quad (16)$$

$$\bullet N_2^* + \bullet O \rightarrow NO + \bullet N \quad (17)$$

$$NO_{(g)} + \bullet O \rightarrow NO_{2(g)} \quad (18)$$

$$3NO_2 + H_2O \rightarrow 2H^+ + 2NO_3^- + NO \quad (19)$$

$$2NO_{2(g)} \rightarrow N_2O_{4(g)} + H_2O_{(l)} \rightarrow HNO_{3(l)} + HNO_{2(l)} \quad (20)$$

$$NO_{2(g)} + NO_{(g)} \rightarrow N_2O_{3(g)} + H_2O_{(l)} \rightarrow 2HNO_{2(l)} \quad (21)$$

$$3HNO_{2(l)} \rightarrow HNO_3 + 2NO_{(g)} + H_2O_{(l)} \quad (22)$$

Equations 11 through 22 delineate the significance of various reactive species, namely •OH, •N, •N_2*, •N_2^+, •H, and •O, in the process of NO_3^- formation. This NO_3^- species subsequently undergoes reactions with hydroxyl radicals and oxygen. When free air is introduced into the reactor, a greater quantity of •OH and •O is generated, with an assumed air composition of 21% oxygen and 79% nitrogen. The generation of •OH during plasma electrolysis predominantly stems from the dissociation of water molecules brought about by electron collisions. The introduction of air containing both oxygen and nitrogen has been found to enhance the production of •OH. This observation aligns with the principle that the presence of oxygen in the injected air contributes to the formation of additional •OH radicals, enhancing the overall reactivity and reaction pathways within the plasma electrolysis system. The increased availability of oxygen, along with other reactive species, promotes the formation of NO and its subsequent interactions, thereby influencing the production of nitrate and other chemical species in the plasma.

4.0 CONCLUSION

This research has successfully demonstrated that plasma electrolysis offers a viable and effective alternative for nitrate synthesis. The study has identified two distinct pathways for nitrate formation: the ammonia pathway, associated with cathodic plasma, and the NO pathway, linked to anodic plasma. These pathways are significantly influenced by the presence and formation of reactive species and intermediates. The introduction of nitrogen injection contributes to the presence of key reactive species, including $\bullet N_2^*$, $\bullet N_2^+$, and •N. The formation of the NO compound can subsequently undergo oxidation to yield NO_2. Furthermore, the reaction between NO_2 and •OH leads to the formation of nitrate. Importantly, any nitrite formed during this process promptly reacts with •OH, resulting in the rapid formation of a more stable compound, which ultimately leads to an increase in nitrate production. The potential mechanism for the formation of •N and •H to produce nitrate via the ammonia pathway involves intricate chemical reactions that are driven by reactive species interactions. This pathway relies on the involvement of •H and •N, as well as the dissosiation process of NH_2 into NH_3, which plays a crucial role in the production of nitrate. The contribution of this research is an environmentally friendly alternative plasma electrolysis technology without CO_2 emissions in fertilizer synthesis. Novelty lies in the role of the anode and cathode in plasma formation so that optimization of the formation of both nitrate and ammonia fertilizer can be identified. Future research is expected to examine other aspects that can increase the production of nitrate and ammonia using the plasma electrolysis method.

Acknowledgment

Thank you to LPPM Universitas Negeri Semarang for funding with the 2023 Domestic Matching Grant Cooperation Research Scheme.

References

[1] A. Wu, J. Lv, X. Xuan, J. Zhang, A. Cao, M. Wang, *et al.*, 2023. "Electrocatalytic disproportionation of nitric oxide toward efficient nitrogen fixation," *Advanced Energy Materials.* 13: 2204231,

[2] K. H. R. Rouwenhorst, P. M. Krzywda, N. E. Benes, G. Mul, and L. Lefferts, 2020. "Ammonia production technologies," *Techno-Economic Challenges of Green Ammonia as Energy Vector*. 41-84.

[3] M. El-Shafie and S. Kambara, 2023. "Recent advances in ammonia synthesis technologies: Toward future zero carbon emissions," *International Journal of Hydrogen Energy*. 48: 11237-11273.

[4] K. Minamisawa, 2023. "Mitigation of greenhouse gas emission by nitrogen-fixing bacteria," *Bioscience, Biotechnology, and Biochemistry*. 87: 7-12.

[5] S. F. Harianingsih, E. Karamah, and N. Saksono, 2021. "Air plasma electrolysis method for synthesis of liquid nitrate fertilizer with K2HPO4 and K2SO4 electrolytes," *International Journal of Plasma Environmental Science and Technology*. 15: e01005,

[6] E. Karamah and N. Saksono, 2021. "Spectroscopic of Radicals Formed and Nitrate Production by Contact Glow Discharge Air Plasma Electrolysis," in *IOP Conference Series: Materials Science and Engineering*. 012092.

[7] C. Chen, Y. Lu, J. Liang, L. Wang, and J. Fang, 2023. "Roles of nitrogen dioxide radical (• NO2) in the transformation of aniline by sulfate radical and hydroxyl radical systems with the presence of nitrite," *Chemical Engineering Journal*, 451: 138755.

[8] K. Kučerová, Z. Machala, and K. Hensel, 2020. "Transient spark discharge generated in various N 2/O 2 gas mixtures: Reactive species in the gas and water and their antibacterial effects," *Plasma Chemistry and Plasma Processing*, 40: 749-773,

[9] M. Keshavarzzadeh, R. Zahedi, R. Eskandarpanah, S. Qezelbigloo, S. Gitifar, O. N. Farahani, et al., 2023. "Estimation of NOx pollutants in a spark engine fueled by mixed methane and hydrogen using neural networks and genetic algorithm," *Heliyon.* 9.

[10] S. Li, H. Shang, Y. Tao, P. Li, H. Pan, Q. Wang, et al., 2023. "Hydroxyl Radical‐Mediated Efficient Photoelectrocatalytic NO Oxidation with Simultaneous Nitrate Storage Using A Flow Photoanode Reactor," *Angewandte Chemie.* e202305538.

[11] B. Farawan, R. D. Yusharyahya, M. Gozan, and N. Saksono, 2021. "A novel air plasma electrolysis with direct air injection in plasma zone to produce nitrate in degradation of organic textile dye," *Environmental Progress & Sustainable Energy*. 40: e13691,

[12] Y. Luo, H. Jiang, L.-X. Ding, S. Chen, Y. Zou, G.-F. Chen, et al., 2023. "Selective Synthesis of Either Nitric Acid or Ammonia from Air by Electrolyte Regulation in a Plasma Electrolytic System," *ACS Sustainable Chemistry & Engineering*. 13(2).

[13] N. Saksono, Harianingsih, B. Farawan, V. Luvita, and Z. Zakaria, 2023. "Reaction pathway of nitrate and ammonia formation in the plasma electrolysis process with nitrogen and oxygen gas injection," *Journal of Applied Electrochemistry*, 1-9.

[14] S. Farisah and N. Saksono, 2021. "Effect of solution pH and conductivity on nitrate synthesis by air contact glow discharge electrolysis method," in IOP Conference Series: *Materials Science and Engineering.* 012091.

[15] K. P. Bhatt, S. Patel, D. S. Upadhyay, and R. N. Patel, 2022. "A critical review on solid waste treatment using plasma pyrolysis technology," *Chemical Engineering and Processing-Process Intensification*, 177: 108989.

[16] M. van de Kerkhof, A. M. Yakunin, V. Kvon, S. Cats, L. Heijmans, M. Chaudhuri, et al., 2021. "Plasma-assisted discharges and charging in EUV-induced plasma," J*ournal of Micro/Nanopatterning Materials, and Metrology*, 20: 013801-013801.

[17] T. Sakakura, Y. Takatsuji, M. Morimoto, and T. Haruyama, 2020. "Nitrogen fixation through the plasma/liquid interfacial reaction with controlled conditions of each phase as the reaction locus," *Electrochemistry,* 88: 190-194.

[18] V. T. Nguyen, D. K. Dinh, N. M. Lan, Q. H. Trinh, M. M. Hossain, V.-D. Dao, et al., 2023. "Critical role of reactive species in the degradation of VOC in a plasma honeycomb catalyst reactor," *Chemical Engineering Science*, 276: 118830.

[19] H. Jin, S. S. Kim, S. Venkateshalu, J. Lee, K. Lee, and K. Jin, 2023. "Electrochemical Nitrogen Fixation for Green Ammonia: Recent Progress and Challenges," *Advanced Science*. 2300951,

[20] H. Sun, N. Jiang, J. Ren, X. Wei, G. Yu, and J. Li, 2023. "Power dependence of reactive species generation in a water falling film dielectric barrier discharge system," *Separation and Purification Technology*. 305: 122406.

[21] E. Vervloessem, M. Gromov, N. De Geyter, A. Bogaerts, Y. Gorbanev, and A. Nikiforov, 2023. "NH3 and HNO x Formation and Loss in Nitrogen Fixation from Air with Water Vapor by Nonequilibrium Plasma," *ACS Sustainable Chemistry & Engineering*. 11: 4289-4298.

[22] H. Jiang, G.-F. Chen, O. Savateev, and H. Wang, 2023. "Visualizing the reaction interface of lithium-mediated nitrogen fixation," *Joule.* 7: 253-256.

[23] T. Zhang, R. Zhou, S. Zhang, R. Zhou, J. Ding, F. Li, et al., 2023. "Sustainable ammonia synthesis from nitrogen and water by one‐step plasma catalysis," *Energy & Environmental Materials.* 6: e12344.

[24] Z. Huang, A. Xiao, D. Liu, X. Lu, and K. Ostrikov, 2022. "Plasma‐water‐based nitrogen fixation: Status, mechanisms, and opportunities," *Plasma Processes and Polymers.* 19: 2100198.

[25] M. P. Rayaroth, C. T. Aravindakumar, N. S. Shah, and G. Boczkaj, 2022. "Advanced oxidation processes (AOPs) based wastewater treatment-unexpected nitration side reactions-a serious environmental issue: A review," *Chemical Engineering Journal*. 430: 133002.

[26] M. Tanski, R. Barbucha, J. Mizeraczyk, and S. Tofil, 2020. "Imaging and emission spectroscopy of the submicrosecond plasma generated from copper substrate with nanosecond laser pulses," *Applied Optics*. 59: 8388-8394.

[27] Y. Tsuchida, N. Murakami, T. Sakakura, Y. Takatsuji, and T. Haruyama, 2021. "Drastically increase in atomic nitrogen production depending on the dielectric constant of beads filled in the discharge space," *ACS Omega*. 6: 29759-29764.